



# Flavor matching of double parton distribution functions

Aron Mees van Kampen, University of Antwerp, Belgium

September 5, 2018

Supervisor: Markus Diehl

Theory group

## Abstract

The goal of this project is to support the flavor matching procedure in the `c++` code `chilipdf` from scratch for the evolution of double parton density functions. To manage this, several functions and classes had to be added. A matching formula for  $\alpha_s$  has to be implemented in the `Alpha_s` class. Kernel matching functions are imported and the matching procedure of PDFs in the VFNS (variable flavor number scheme) has been implemented in another class. All these feature functions have been tested. Results and comments on these tests can be found in this report.

# Contents

<b>1. Introduction</b>	<b>3</b>
1.1. QCD, PDFs & DPDs . . . . .	3
<b>2. Theory</b>	<b>5</b>
2.1. Variable Flavor Number Scheme . . . . .	5
2.2. Matching of $\alpha_s$ . . . . .	6
2.3. Flavor matching . . . . .	7
<b>3. Flavor matching in c++</b>	<b>8</b>
3.1. Operator matrix elements . . . . .	8
3.2. Structure of the flavor matching procedure . . . . .	9
<b>4. Results</b>	<b>11</b>
4.1. $\alpha_s$ matching . . . . .	11
4.2. Flavor matching . . . . .	14
4.3. Other tests and subtleties . . . . .	17
4.3.1. Maple versus c++; trilogarithm . . . . .	17
4.3.2. Mellin moments . . . . .	17
<b>5. Conclusion</b>	<b>18</b>
<b>A. VFNS comparison with Benchmark results</b>	<b>21</b>

# 1. Introduction

The Large Hadron Collider (LHC) is currently operating at a centre of mass energy of 13 TeV, this could increase with coming upgrades and with new hadron colliders, for example the FCC (Future Circular Collider) which would run at energies of about 100 TeV. At these high energies the densities of partons (quarks and gluons) inside the proton are very large and the gluon density is typically dominant. For a more accurate theoretical (Monte Carlo) simulation of proton-proton collisions at these energies, one can involve multi-parton interactions (MPI) in the calculations. In a single parton interaction there are two partons that interact in the hard scatter, while in a multi parton interaction two of such hard scattering interactions take place (i.e. four partons interact).

## 1.1. QCD, PDFs & DPDs

Quantumchromodynamics (QCD) is the quantum field theory of the non-abelian group SU(3) which is used for the description of the strong interaction in the standard model of elementary particle physics. The fundamental parameters of this theory are scale- ( $Q$ , or mostly indicated by the renormalization scale:  $\mu$ ) dependent as a result of renormalization. Here, we concentrate on two scale dependent quantities: the strong coupling  $\alpha_s(\mu)$  and parton density functions (PDFs)  $f_i(x, \mu)$ . The dependence of  $\alpha_s$  to the scale can be described elegantly by the renormalization group equation or the beta-function  $\beta(\alpha_s)$ . The scale dependence of  $\alpha_s$  has been confirmed experimentally, which can be seen in figure 1. For QCD with  $n_F < 16$  color charged fermionic fields (quark flavors), the beta-function is negative and dictates a decreasing coupling for increasing energy scales. In the standard model there are  $n_F = 6$  quark flavors.

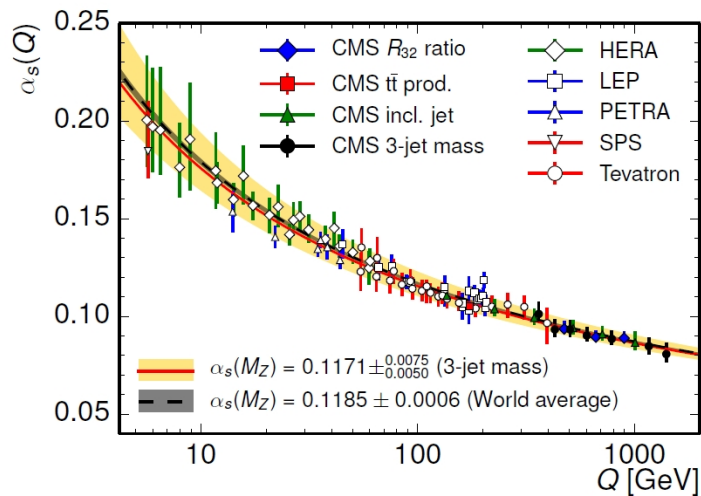


Figure 1: Measurements of  $\alpha_s$  at different energies confirm the running of the strong coupling. [3]

To calculate cross sections of single hard processes, the non-perturbative low scale has to be separated from the perturbative high scale part. A general cross section can be factorized as:

$$\sigma = \sum C \otimes A \quad (1)$$

where  $C$  are coefficient functions and  $A$  represents the partonic part of the cross section. The hard and soft scales are separated by the factorization scale  $\mu_F$ . The separation of high scale and low scale dynamics is accomplished by the operator product expansion (OPE). This factorizes highly singular operators into regular, local operators and coefficient functions.

The OPE has to be renormalized to remove the UV divergences, and therefore the operators become scale dependent. The low scale dynamics information of the partons inside the proton is contained by the non-perturbative hadronic operator matrix elements (OMEs). PDFs can be distracted from OMEs (using the Mellin convolution). They depend on Björken  $x$  and the scale  $\mu$ . The dependence of the PDFs to the renormalization scale  $\mu$  - evolution - can be described in a rigorous way by the DGLAP (Dokshitzer-Gribov-Lipatov-Altarelli-Parisi) evolution equations which can be written in a compact form like:

$$\frac{\partial}{\partial \log(\mu)} f_i(x, \mu) = \sum_j P_{ij} \otimes f_j(x, \mu) \quad (2)$$

where  $P_{ij}$  are the splitting functions.

The factorization theorem for a double parton interaction in double Drell-Yan production most likely holds. There is a lot of progress in the proof of this, see [2]. The calculation of the double parton scattering within this framework makes use of so-called double patron distribution functions (DPDs). These are noted by  $f_{ij}(x_i, x_j; \mu_1, \mu_2)$ . DPDs fulfill evolution equations that are very similar to the DGLAP equations for single PDFs. The aim is to produce DPDs from experimental results to make better predictions of QCD phenomena.

`chlipdf` is an evolution code for DPDs and is currently in full development. It is build from scratch in the `c++` language. In the current state of the development, the functions have structures that are only applicable on single PDFs. In this project, it is aimed to treat the problem of matching of PDFs (or DPDs). This is necessary in an effective field theory for energy scales under quark masses. The heavy quark effective theory treats the heavy quarks with masses above the QCD mass scale ( $\sim 200$  MeV) non-perturbatively. The quark masses that are larger than the chosen energy scale are treated like infinite masses. For larger energy scales, there are more light quarks  $n_f$  to be taken into account. This changes the fundamental parameters and functions slightly. That is why matching of the coupling  $\alpha_s$  and of the PDFs has to be implemented in an evolution code such as `chlipdf`.

## 2. Theory

Several aspects of implementing the heavy quark thresholds to the DPD evolution are clarified in this section. The variable flavor number scheme (VFNS) is the main tool that is used for the right procedures of matching  $\alpha_s$  and the PDFs. Unlike the fixed flavor number scheme (FFNS), the VFNS takes the masses of the quarks into account.

### 2.1. Variable Flavor Number Scheme

The VFNS is a renormalization scheme which works parallel to the modified minimal subtraction ( $\overline{\text{MS}}$ ) scheme, with the difference that this scheme involves sub-schemes that are parameterized by the number of active (light) quarks  $n_f$ . The heavy flavors decouple from the light quarks in this procedure. The only region where this is effective, is for quark thresholds above the QCD scale  $\Lambda_{\text{QCD}} \propto 200 - 300 \text{ MeV}$ . Consequently the 3 lightest quarks (u, d, s)<sup>1</sup> are not thresholds that have to be passed in matching, because these quarks are produced non-perturbatively. The PDFs that are assigned to light quarks (and the gluon) treat them as massless particles and describe the non-perturbative features. The heavy quark has flavor number  $(n_f+1)$ . This quark does not appear in tree level diagrams, but it can appear in the form of radiative corrections (virtual).

To merge the sub-schemes into a continuous scheme that contains the whole range of evolution  $[\mu_0, \mu]$ , one needs a matching scale  $\mu_m$  for every merge of two sub-schemes. The new PDFs with  $n_f + 1$  flavors are calculated in terms of the old PDFs of the  $n_f$  scheme and  $\alpha_s^{(n_f)}(\mu_m)$ . The matching scale is usually chosen to be the heavy quark mass ( $m_h$ ). This choice is convenient because the terms in the matching conditions that contain the logarithmic factor  $\ln(m_h^2/\mu_m^2)$  will vanish. An illustration of four sub-schemes with their corresponding  $n_f$  is given in figure 2. In Figure-a the matching scale is equal to the heavy quark mass.

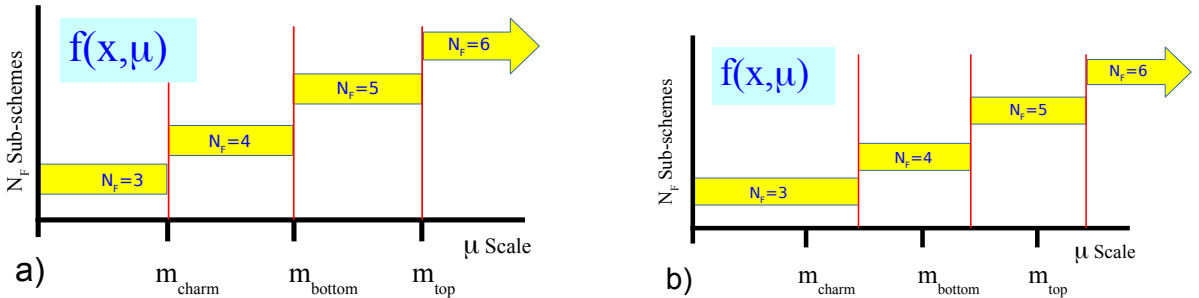


Figure 2: Matching scheme configurations. In Figure-a the matching scales are chosen at the heavy quark masses, in Figure-b the matching scales are larger. [5]

<sup>1</sup>With  $\overline{\text{MS}}$  masses respectively:  $m_u = 2.2 \text{ MeV}$ ,  $m_d = 4.7 \text{ MeV}$ ,  $m_s = 95 \text{ MeV}$  [4]

PDFs for the individual quark flavors exist in the parton basis, i.e. every parton  $i$  has its own density function  $f_i(x, \mu^2)$ . The scale evolution of PDFs is executed in a different basis, called the evolution basis. In this basis there are three types of PDFs: the non-singlet densities  $\Delta_k^\pm(x, \mu^2, n_f)$ , singlet densities  $\Sigma^\pm(x, \mu^2, n_f)$  and the gluon density  $G(x, \mu^2, n_f)$ . They are linear combinations of the parton based functions as follows:

$$\Delta_k^\pm(x, \mu^2, n_f) = f_k(x, \mu^2, n_f) \pm f_{k+1}(x, \mu^2, n_f) \quad (3)$$

$$f_k^{NS,\pm}(x, \mu^2, n_f) = \Delta_k^\pm(x, \mu^2, n_f) - \Delta_{k+1}^\pm(x, \mu^2, n_f) \quad (4)$$

$$\Sigma(x, \mu^2, n_f) = \sum_{k=1}^{n_f} [f_k(x, \mu^2, n_f) + f_{\bar{k}}(x, \mu^2, n_f)] \quad (5)$$

$$G(x, \mu^2, n_f) = g(x, \mu^2, n_f) \quad (6)$$

The non-singlet and singlet PDFs consist only of combinations of quark densities (the summation index  $k$  runs over active quark flavors). In the matching and evolution procedures the gluon does mix with the singlet  $\Sigma^+$  combination.

## 2.2. Matching of $\alpha_s$

The Callan-Symanzik beta-function of QCD describes the  $\mu$  dependence of  $\alpha_s$ . Both the beta-function and  $\alpha_s$  depend on the number of active quark flavors. The beta-function can be calculated perturbatively and therefore also  $\alpha_s$  can. The calculation of the matching relation between  $\alpha_s^{(n_f)}$  and  $\alpha_s^{(n_f-1)}$  comes down to calculating all the loop-diagrams that contain the heavy quark (with flavor number  $n_f$ ) till certain order to renormalize the coupling constant. In [6] this is done for three loops in the  $\overline{\text{MS}}$  scheme. The result to second order (NNLO) of this calculation is cited here, where  $a = a^{(n_f)}(\mu^{(n_f)}) = \alpha_s^{(n_f)}/\pi$  and  $a' = a^{(n_f-1)}(\mu^{(n_f)})$ :

$$\frac{a'}{a} = 1 - \frac{l_h}{6}a + \left( \frac{l_h^2}{36} - \frac{19}{24}l_h + \frac{11}{72} \right) a^2 + \mathcal{O}(a^3) \quad (7)$$

where  $l_h = \ln \left[ \frac{(\mu^{(n_f)})^2}{\mu_h^2} \right]$ , with  $\mu_h$  the  $\overline{\text{MS}}$  mass of the heavy quark. This is the equation for matching to lower scales (matching down).

For the matching to higher scales, one needs the inverse of equation 7. This is accomplished with a series inversion [7]. The inverted function for NNLO is:

$$\frac{a}{a'} = 1 + \frac{l_h}{6}a' + \left( \frac{l_h^2}{36} - \frac{19}{24}l_h - \frac{11}{72} \right) a'^2 + \mathcal{O}(a^3) \quad (8)$$

To cover all possible choices of the user of `chilipdf`, the matching formulas for  $\alpha_s$  should also be implemented for the usage of the pole mass ( $M_h$ ) instead of the  $\overline{\text{MS}}$  mass ( $\mu_h$ ) for the heavy quark. The pole mass is the experimentally measured mass of a particle. The name originates from the fact that the propagator has a pole at the pole mass value. The  $\overline{\text{MS}}$  mass is the renormalized mass that is dependent on the scale. The

assumption for equations 7 and 8 is:  $\mu_h = m_h(\mu_h)$ , the heavy quark mass at the scale of this mass.

It is sufficient to use the relation between  $M_h$  and  $\mu_h$  up till first order in  $\alpha_s$  to find an accurate version of the matching formulas for the pole mass. The relation between the pole mass and the  $\overline{\text{MS}}$  mass is [6]:

$$\frac{\mu_h}{M_h} = 1 - \frac{4}{3} \frac{a(M_h)}{\pi} \quad (9)$$

The matching relation for  $\alpha_s$  with the usage of the pole mass becomes:

$$\frac{a'}{a} = 1 - \frac{\mathcal{L}_h}{6} a + \left( \frac{\mathcal{L}_h^2}{36} - \frac{19}{24} \mathcal{L}_h - \frac{7}{24} \right) a^2 + \mathcal{O}(a^3) \quad (10)$$

where  $\mathcal{L}_h = \ln \left[ \frac{(\mu^{(n_f)})^2}{M_h^2} \right]$ . The inverse is similar to equation 8, instead of the last factor  $\frac{11}{72} a^2$  this is  $-\frac{7}{24} a^2$ .

### 2.3. Flavor matching

In a scheme with  $n_f + 1$  flavors, the heavy quark (quark number  $n_f + 1$ ) is treated as completely massless. The scale evolution of this PDF behaves like the evolution with  $n_f + 1$  massless quarks. In a scheme with  $n_f$  flavors, this specific quark is not treated as massless. The connection between the  $n_f$ -flavor and  $(n_f+1)$ -flavor schemes is established by the equalization of both schemes at the matching scale  $\mu$ . Therefore one has to factorize the Wilson coefficients in massless Wilson coefficients  $\mathcal{C}_{i,a}$  and massive operator matrix elements (OMEs)  $A_{ij}$ . The heavy quark OMEs ( $A_{Qj}$  and  $A_{ij,Q}$ )<sup>2</sup> are the kernels for the matching relations of PDFs. These objects are free from collinear divergences [9]:

$$A_{Qj} \left( n_f, \frac{\mu^2}{m^2} \right) = \langle j(p) | O_Q(0) | j(p) \rangle \quad (11)$$

with  $O_Q(0)$  the renormalized operator from the operator product expansion of two electromagnetic currents near the light cone [9]. The quantities  $A_{ij,Q} \left( n_f, \frac{\mu^2}{m^2} \right)$  represent the heavy-quark-loop contributions to the light-quark and gluon OMEs and are defined in the same manner as equation 11 but with the operator  $O_l(0)$  with  $l = q, g$ . The explicit form of these kernels are given in the appendices of [9], [10], [11] and [12]. The matching relations for the PDFs in the evolution basis are:

$$f_k^{NS}(n_f + 1) = A_{qq,Q}^{NS}(n_f + 1) f_k^{NS}(n_f) + \frac{1}{n_f} A_{qq,Q}^{PS}(n_f + 1) \Sigma(n_f) + \frac{1}{n_f} A_{gg,Q}^S(n_f + 1) G(n_f) \quad (12)$$

$$G(n_f + 1) = A_{gg,Q}^S(n_f + 1) \Sigma(n_f) + A_{gg,Q}^S(n_f + 1) G(n_f) \quad (13)$$

---

<sup>2</sup>The notation of the heavy quark as  $Q$  in this report is based on the notation in [10]

$$\begin{aligned}\Sigma(n_f + 1) &= \left[ A_{qq,Q}^{NS}(n_f + 1) + A_{qq,Q}^{PS}(n_f + 1) + A_{Qq}^{PS}(n_f + 1) \right] \Sigma(n_f) \\ &\quad + \left[ A_{qg,Q}^S(n_f) + A_{Qg}^S(n_f) \right] G(n_f)\end{aligned}\tag{14}$$

where NS is non-singlet, S is singlet and PS = S - NS is pure singlet. These expressions are taken from [13]. They are general and defined without order. The matching equations simplify in our case because some kernels are zero to first or second order. The simplified and factorized formulas are:

$$f_k^{NS,\pm}(n_f + 1) = f_k^{NS,\pm}(n_f) + \left( \frac{\alpha_s}{4\pi} \right)^2 A_{qq,Q}^{NS,(2)} \otimes f_k^{NS,\pm}(n_f)\tag{15}$$

$$\begin{aligned}G(n_f + 1) &= \left[ 1 + \left( \frac{\alpha_s}{4\pi} \right) A_{gg,Q}^{S,(1)} + \left( \frac{\alpha_s}{4\pi} \right)^2 A_{gg,Q}^{S,(2)} \right] \otimes G(n_f) \\ &\quad + \left( \frac{\alpha_s}{4\pi} \right)^2 A_{gg,Q}^{S,(2)} \otimes \Sigma(n_f)\end{aligned}\tag{16}$$

$$\begin{aligned}\Sigma^+(n_f + 1) &= \left[ 1 + \left( \frac{\alpha_s}{4\pi} \right)^2 \left( A_{qq,Q}^{NS,(2)} + A_{Qq}^{PS,(2)} \right) \right] \otimes \Sigma^+(n_f) \\ &\quad + \left[ \left( \frac{\alpha_s}{4\pi} \right) A_{Qg}^{S,(1)} + \left( \frac{\alpha_s}{4\pi} \right)^2 A_{Qg}^{S,(2)} \right] \otimes G(n_f)\end{aligned}\tag{17}$$

$$\Sigma^-(n_f + 1) = \left[ 1 + \left( \frac{\alpha_s}{4\pi} \right)^2 A_{qq,Q}^{NS,(2)} \right] \otimes \Sigma^-(n_f)\tag{18}$$

$$\begin{aligned}f_{n_f}^{NS,+} f_{n_f+1}^{NS,+}(n_f + 1) &= f_{n_f}^{NS,+}(n_f + 1) - \left[ \left( \frac{\alpha_s}{4\pi} \right) A_{Qg}^{S,(1)} + \left( \frac{\alpha_s}{4\pi} \right)^2 A_{Qg}^{S,(2)} \right] \otimes G(n_f) \\ &\quad - \left( \frac{\alpha_s}{4\pi} \right)^2 A_{Qq}^{PS,(2)} \otimes \Sigma(n_f)\end{aligned}\tag{19}$$

$$f_{n_f}^{NS,-} f_{n_f+1}^{NS,-}(n_f + 1) = f_{n_f}^{NS,-}(n_f + 1)\tag{20}$$

where  $f_{n_f}^{NS}$  means the heaviest non singlet PDF from the set with  $n_f$  light quarks. And  $f_{n_f+1}^{NS}$  is the heaviest non singlet PDF from the new set with  $n_f + 1$  light quarks.

## 3. Flavor matching in c++

### 3.1. Operator matrix elements

The matching OMEs ( $A_{ij,Q}$  and  $A_{Qj}$ ) that are needed for the matching up to NNLO are functions of the Björken variable<sup>3</sup>  $z$ , the heavy quark mass  $m_h$  and the matching scale  $\mu$ . The scale and heavy quark mass only appear in the logarithmic factor  $L_M = \ln \left( \frac{m_h^2}{\mu^2} \right)$ . The matching kernels do not depend on  $n_f$ .

To implement the kernel functions in a correct way, the first check is to compare the functions that are given in [9] with the same functions in [10], [11] and [12] and verify

---

<sup>3</sup>Noted as  $x$  in [10]



if they give the same results for general values of  $z$  and  $L_M$ . This is done in a `Maple` sheet. The entered functions in `Maple` made it possible to shorten the functions a bit. Primarily some polynomials and logarithms could be merged. This is also used as a method to check which form of the two was the shortest one, dependent on the amount of (logarithmic) multiplications.

In the matching kernels, harmonic polylogarithms [14] are used. These functions - noted as  $H_{a,\vec{b}}$  - are a generalization of Nielsen's polylogarithms. Both are combinations of polylogarithms:

$$\text{Li}_n(z) \equiv \sum_{k=1}^{\infty} \frac{z^k}{k^n}$$

From the check with `Maple`, it could be concluded that the usage of harmonic polylogarithms is more economical than the usage of ordinary polylogarithms.

To be able to do the multiplication of a matching function with a PDF (which is a vector), the kernels have to be transformed to a matrix. This procedure is already implemented in the code. To make sure that this procedure works, the function has to be divided in pieces depending on their degree of singularity. The general structure of a kernel can be written down as:

$$\begin{aligned} A\left(z, \frac{m}{\mu}\right) &= A_{reg}\left(z, \frac{m}{\mu}\right) + A_+\left(z, \frac{m}{\mu}\right) + A_\delta\left(z, \frac{m}{\mu}\right) \delta(1-z) \\ &= \text{regular} + \text{singular} + \text{singular\_integral} \end{aligned} \quad (21)$$

The regular part does not contain singularities in  $z$ . The  $\delta$  part has to be integrated and is fully added to the `singular\_integral` part. The term with the  $+$  needs the treatment of the plus-description. Then some terms with  $\delta$ -function appear which end up in `singular\_integral` and the rest can be divided in terms that are singular (terms with  $\ln(z)$  or powers of  $1/z$ ) and terms that are regular (including terms with  $\ln(z)/z$ ).

After entering the matching kernels in a class in `c++` the outcome of this can be compared to the outcome of the `Maple` file(s). This test is performed for the second order terms of the kernels without factors of  $\alpha_s$  in `test_matching.cpp`. The first order terms are not being checked because they are very short.

### 3.2. Structure of the flavor matching procedure

The implementation of the necessary parts of flavor matching requires 3 classes in the code: `"Matching"`, `"Matching_matrices"` and `"Flavor_conversion"`. Here the contents of the classes is shortly clarified.

In the `Matching` class the kernel functions are coded. Two first order kernels:  $A_{gg,Q}^{S,(1)}$ ,

$A_{Qg}^{S,(1)}$  and five second order kernels:  $A_{Qg}^{S,(2)}$ ,  $A_{gg,Q}^{S,(2)}$ ,  $A_{Qq}^{PS,(2)}$ ,  $A_{qq,Q}^{NS,(2)}$ ,  $A_{gg,Q}^{S,(2)}$ . The multiplications with powers of  $\alpha_s$  is done in a later step because of the formation of common combinations. Powers of logarithms that appear often are defined as `const double` to reduce the calculation time. In this class, the division of regular, singular and singular\_integral parts is applied. In this way, it can be passed to the `kernel_matrix` class to form matrices. The arguments of the functions are  $y = 1 - z$  and a set of parameters. The only parameter needed is the logarithm of the heavy quark mass divided by the matching scale. Using  $1 - z$  instead of  $z$  facilitates a more accurate value of the logarithms for  $z \rightarrow 1$ . The logarithm of  $z$  is then calculated as:  $\ln(z) = \text{log1p}(-y)$ . This function is more accurate to calculate the logarithm for arguments close to 1 (where the logarithm becomes 0).

In "Matching\_matrices" the matrices are formed and combined in a way that matches with equations 15 - 20. The constructor of this class automatically makes the matrices and stores them in a container. The arguments of the constructor are  $L_M$ , the order of the matching, the mass type ( $\overline{\text{MS}}$  mass or pole mass) and the Chebyshev grid on which the kernel matrices are constructed. The grid is the same grid on which the PDF is interpolated. The name originates from Chebyshev interpolation [15]. The mass type is a necessary enum for making the matching kernels that have both a NLO and a NNLO part. The only factor in which the heavy quark mass appears is in the logarithm  $L_M$ . The correction for using the  $\overline{\text{MS}}$  mass instead of the pole mass is equal to:

$$\ln\left(\frac{M_h}{\mu}\right) = \ln\left(\frac{\mu_h}{\mu}\right) + \frac{4}{3}\left(\frac{\alpha_s}{4\pi}\right) + \frac{8}{9}\left(\frac{\alpha_s}{4\pi}\right)^2 \quad (22)$$

where  $M_h$  is the pole mass and  $\mu_h$  is the  $\overline{\text{MS}}$  mass. This only leads to new NNLO terms if there is a NLO term in the same kernel. All the other multiplications give terms of  $\mathcal{O}(\alpha_s^3)$ .

The "Flavor\_conversion" class applies equations 15 - 20 to a PDF set. To match only the non-singlet combinations that are defined in the specific scheme, the function loops over all active ( $n_f$ ) non-singlet PDFs. Also new non-singlet PDFs that contain the heavy quark ( $qQ^\pm$ ) must be added.

The constructor of this class makes an object of `Matching_matrices`, which contains a container with all necessary matrices for the given order. It also calculates  $L_M$  using the argument  $\frac{m_h}{\mu}$ . When the constructor is called, one can match a PDF from  $n_f$  light quarks to  $n_f + 1$  light quarks with the function `PDFset_nFp1`. This function has the arguments: the old PDF set, the new PDF set, the matching scale  $\mu$  and an object of the `Alpha_s` class. In this function, first the related  $n_f$  is checked. Namely the new PDF set should possess  $n_f + 1$  flavors if the old set possesses  $n_f$ . Then the new set PDFs can be calculated according to the matching order using the old set, the (combinations of) kernel matrices and factors of  $\alpha_s/4\pi$ .

## 4. Results

### 4.1. $\alpha_s$ matching

The matching of  $\alpha_s$  is implemented in both directions: matching up (to  $n_f + 1$ ) and matching down (to  $n_f - 1$ ). For a check of the running and matching of  $\alpha_s$  the commonly used starting value is the experimental value at the Z boson mass scale (see [3])  $M_Z = 91.1876$  GeV.

$$\alpha_s(M_Z) = 0.118$$

At this scale, the most logical choice of scheme is the  $n_f = 5$  scheme because the mass of the Z boson is much higher than the bottom quark mass. Matching up from this scale does not make sense currently because energy transfers above the top quark mass are very rare within collisions that take place at the current accelerators.

Checks are done for evolving  $\alpha_s$  from  $\mu = M_Z$  down to  $\mu = 1$  GeV with matching from  $n_f = 5$  to  $n_f = 3$ . The evolution works and was already implemented in the `Alpha_s` class. To observe the effect of matching, different matching scales are chosen and the matching order is varied. For the comparison, the absolute value of  $\alpha_s$  is plotted for a specific scheme or multiple schemes and the relative difference between two schemes is plotted. For example, the relative difference between scheme 1 and scheme 2 is calculated as:

$$\text{Rel. diff.} = 1 - \frac{\alpha_s^{(1)}}{\alpha_s^{(2)}}$$

In figure 3 the matching of  $\alpha_s$  is shown with the choice of matching scales equal to the heavy quark masses ( $\mu_1 = m_b$  and  $\mu_2 = m_c$ ). This means that  $l_h$  in equation 7 is zero and the matching does not cause large changes at the matching scale. The differences between the three perturbative orders (LO, NLO and NNLO) are caused by the change of the beta function when going to higher orders. In figure 4 the relative difference of the NLO and NNLO matching is given. These effects due to matching are visible, but very small.

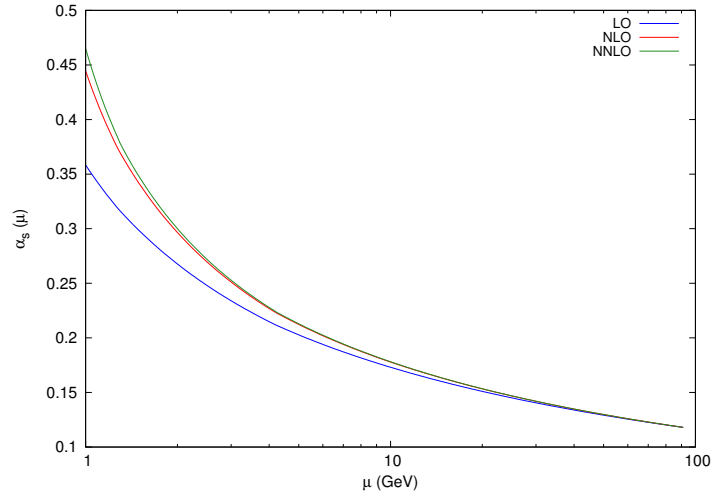


Figure 3: The running of  $\alpha_s$  with matching at the heavy quark masses GeV  $\mu_1 = m_b = 4.18$  GeV and  $\mu_2 = m_c = 1.275$  for LO, NLO and NNLO.

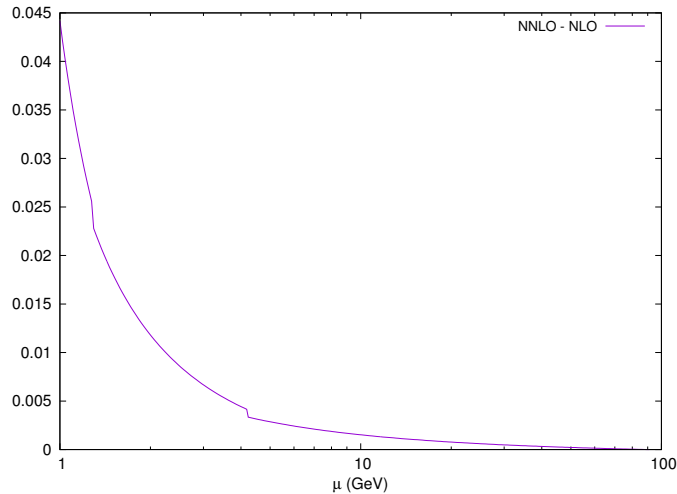


Figure 4: Relative difference between NNLO and NLO. Matched with the matching scales from figure 3.

In the next two figures the same plots are made, but here the matching scales are not equal to the heavy quark masses. The matching scales are  $\mu_1 = 2m_b$  and  $\mu_2 = 2m_c$ . The mass logarithm  $l_h$  is non-zero ( $l_h = \ln(1/2)$ ) so the matching is non-trivial. In the plot with the relative difference between NLO and NNLO (figure 6) the matching points are clearly visible because of the discontinuities.

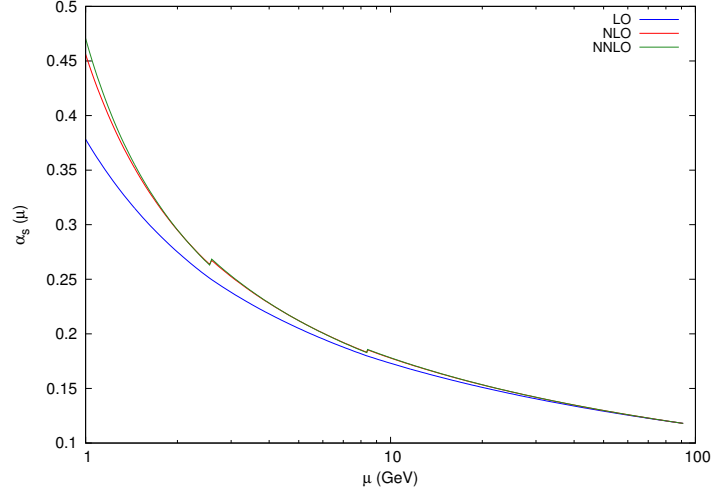


Figure 5: The running of  $\alpha_s$  with matching at twice the heavy quark masses  $\mu_1 = 2m_b$  and  $\mu_2 = 2m_c$  GeV for LO, NLO and NNLO.

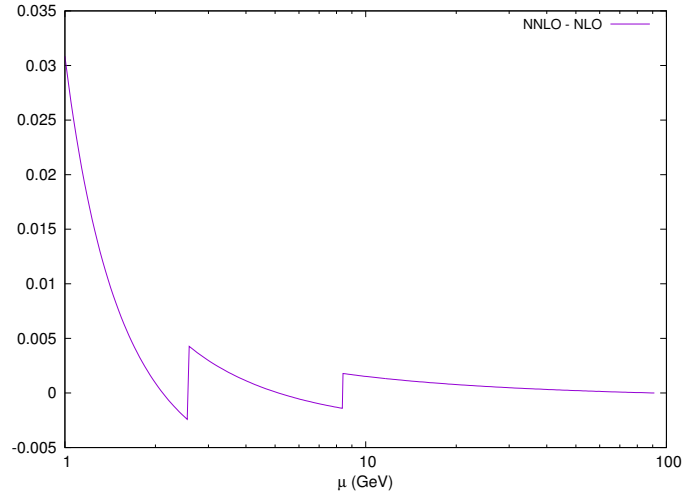


Figure 6: Relative difference between NNLO and NLO matching with matching scales from figure 5.

Finally, comparisons are done for fixed order matching with different matching scales. Again  $\alpha_s$  has been evolved from  $\mu = M_Z$  to  $\mu = 1$  GeV, but only the range  $\mu \in [1, 10]$  GeV is plotted. For one run, the matching scales are set to  $\mu_1 = m_b$ ,  $\mu_2 = m_c$ . For the other run, the matching scales are  $\mu_1 = 2m_b$ ,  $\mu_2 = 2m_c$ . The relative difference between these runs in LO and in NNLO are shown in figure 7 and 8.

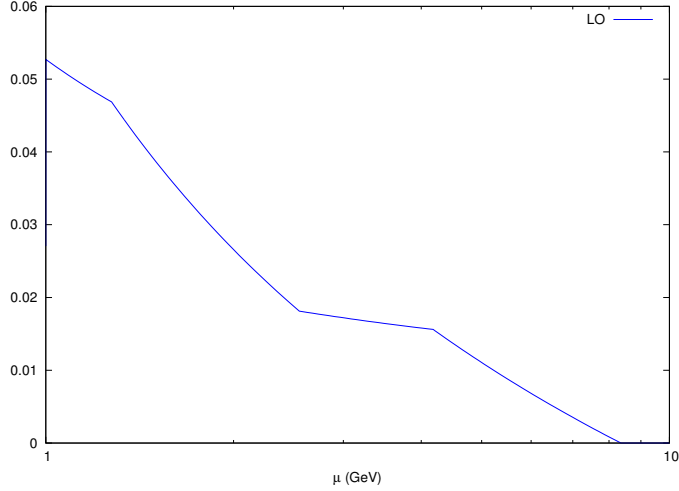


Figure 7: Relative difference of matching at LO with two different matching scales.  
 $\mu_1 = 8.36 \text{ GeV} / 4.18 \text{ GeV}$ .  $\mu_2 = 2.55 \text{ GeV} / 1.275 \text{ GeV}$ .

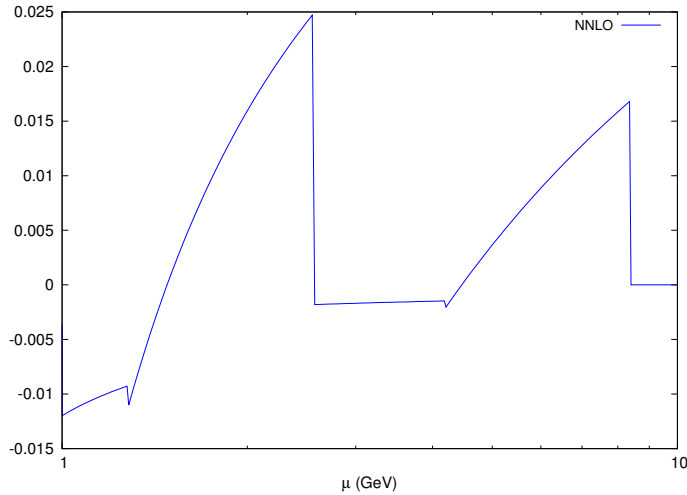


Figure 8: Relative difference of matching at NNLO with two different matching scales.  
 $\mu_1 = 8.36 \text{ GeV} / 4.18 \text{ GeV}$ .  $\mu_2 = 2.55 \text{ GeV} / 1.275 \text{ GeV}$ .

## 4.2. Flavor matching

Firstly the evolution in a VFNS is compared to the exact same evolution with the same starting PDF set, and the same matching scales which has already been done and these Benchmark results are tabled in [16]. The starting PDF set consists of fake data, i.e. these are polynomials that do not represent physical PDFs but are suitable for a good comparison. The relative difference between the matching and evolving procedure from `chilipdf` and the Benchmark results are given in Appendix A.

Secondly, the flavor matching (or implementation of the VFNS) of PDFs is tested against a fixed flavor evolution with  $n_f = 4$ . The starting PDF LesHouchesWG2002 is evolved from  $\mu = \sqrt{2} \text{ GeV}$  to  $\mu = 100 \text{ GeV}$ . The application of the VFNS is executed at two quark thresholds with matching scales at the heavy quark masses:  $m_c = \sqrt{2} \text{ GeV}$  and

$m_b = 4.5$  GeV. The relative difference between the evolved gluon density at the final scale  $\mu = 100$  GeV using the FFNS and the VFNS is shown in figure 9. The same comparison is shown for the evolved u valance quark density in figure 10.

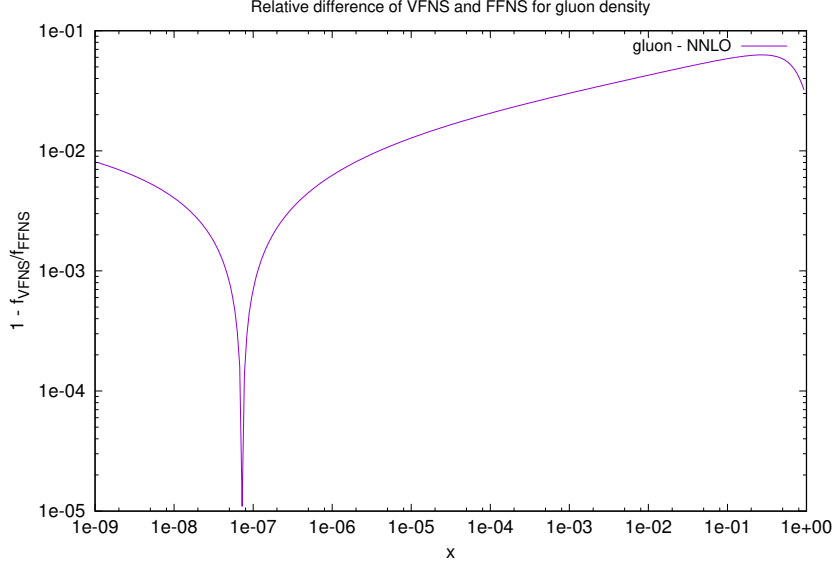


Figure 9: Comparison FFNS ( $n_f = 4$ ) and VFNS ( $n_f = 3$  to 5) for the gluon density at  $\mu = 100$  GeV with NNLO matching and evolution.

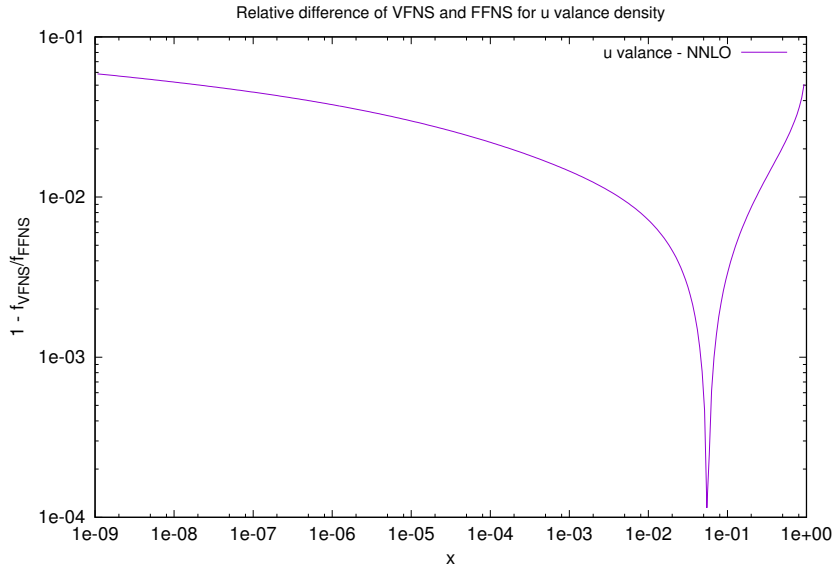


Figure 10: Comparison FFNS ( $n_f = 4$ ) and VFNS ( $n_f = 3$  to 5) for the u valance density ( $u-\bar{u}$ ) at  $\mu = 100$  GeV with NNLO matching and evolution.

Finally, the evolved and matched PDFs are plotted for the three implemented perturbation orders (LO, NLO and NNLO) with error bands that are produced by changing the matching scales. The upper limits of these error bars are produced by matching at twice the heavy quark masses on the one hand and matching at half of the bottom quark mass on the other side. The fat lines represent the PDF that is matched at the

heavy quark masses. So three different combinations of matching scales give the error band:

1.  $\mu_1 = m_c$  &  $\mu_2 = m_b/2$
2.  $\mu_1 = m_c$  &  $\mu_2 = m_b$
3.  $\mu_1 = 2m_c$  &  $\mu_2 = 2m_b$

The evolution range in the two examples given here is  $\mu = \sqrt{2}$  GeV to  $\mu = 100$  GeV and two heavy quark thresholds are passed, namely these of the charm and the bottom quark. The choice of the quark mass values is equal to the choice in [16]:  $m_c = \sqrt{2}$  GeV and  $m_b = 4.5$  GeV. In figure 11 the gluon distribution and in figure 12 the  $c + \bar{c}$  distributions at  $\mu = 100$  GeV are shown.

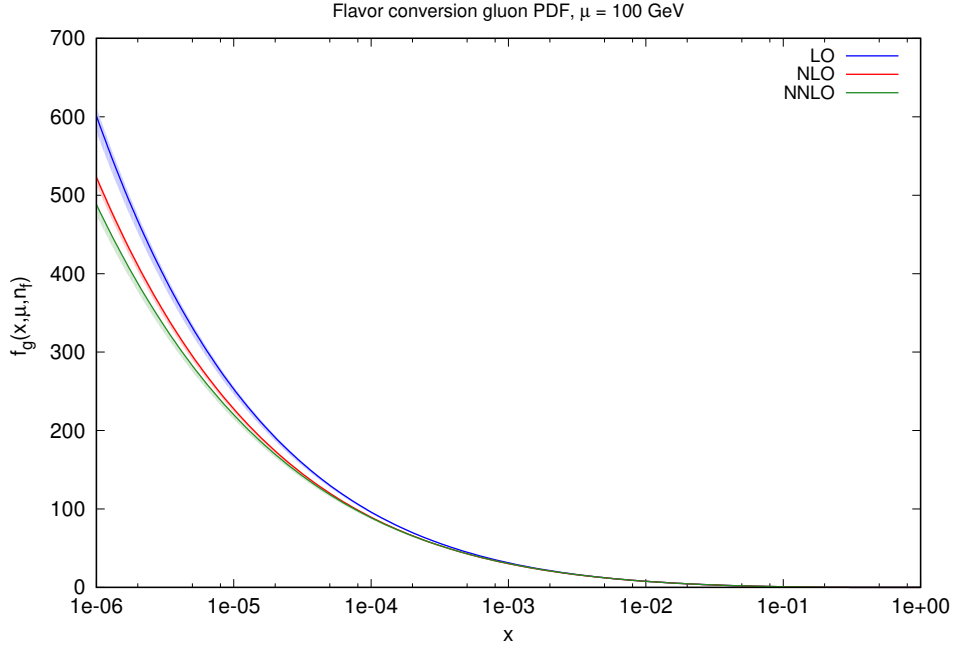


Figure 11: gluon PDF at  $\mu = 100$  GeV. The evolution of the PDF for different matching scales creates an error band for each perturbative order.



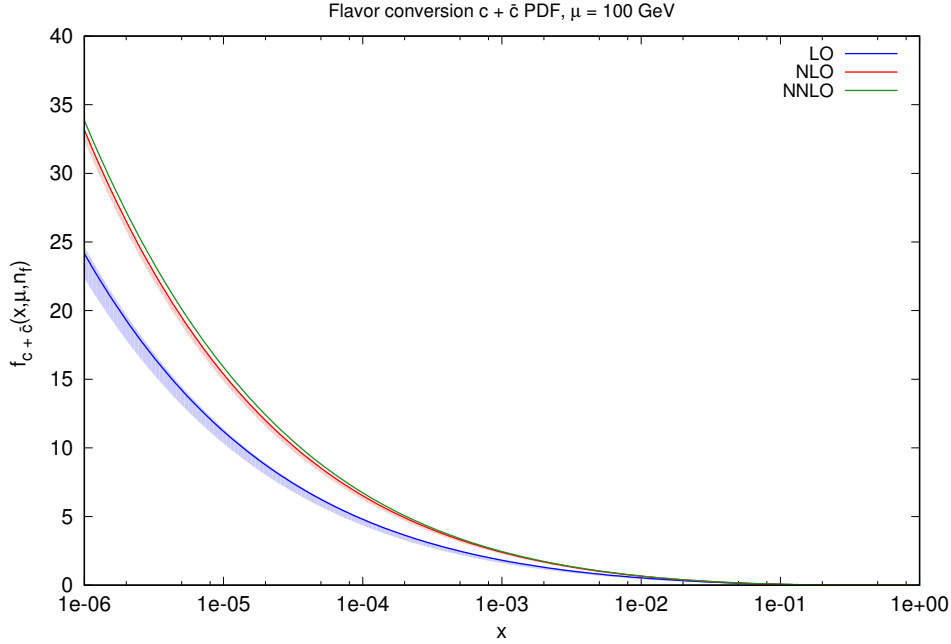


Figure 12: charm + anti-charm quark PDF at  $\mu = 100$  GeV. The evolution of the PDF for different matching scales creates an error band for each perturbative order.

### 4.3. Other tests and subtleties

#### 4.3.1. Maple versus c++; trilogarithm

After some checks between the numerical matching kernel results from `c++` against the `Maple` results it seemed that there were different approaches of the trilog. Therefore a check has been done to compare the `Maple` values against these of the `xmath` implementation of `chilipdf`. Apparently, in `xmath` the trilogarithm with the argument  $-z$  (which is used in one of the matching kernels, namely in  $A_{Qg}^{(2)}$ ) is not accurately calculated. Therefore  $\text{Li}_3(-z)$  has been rewritten with the square relationship<sup>4</sup>:

$$\text{Li}_s(-z) + \text{Li}_s(z) = 2^{1-s} \text{Li}_s(z^2) \quad (23)$$

with this implementation, the matching kernels corresponded with a relative difference to orders of  $10^{-16}$  which is machine precision.

#### 4.3.2. Mellin moments

A check for the matching kernels to be right is to transform them to Mellin space and compare it with the Mellin transformed functions which are also given in the papers [10] and [11].

The Mellin convolution is famous for the simplicity of the operation. Instead of the integral convolution in  $x$  space, one can transform this to a simple multiplication of

<sup>4</sup><https://en.wikipedia.org/wiki/Polylogarithm>

numbers (instead of matrices and vectors). This makes the check rigorous. The check is only done for the  $A_{qq}$  kernel, because it is a short one and at the matching the gluon mixes with all other PDFs in the evolution basis. It is also one of the fewer kernels that contains regular, singular and singular\_integral parts.

## 5. Conclusion

The matching of  $\alpha_s$  is implicitly verified by comparing the values with the Benchmark values at the same scales. This seems to agree on a high accuracy. There are still some slight doubts whether the implementation of the matching kernels and the combining of the matrices is done at the exactly right way. The tests that are done give a signal that it is not far off. But still, the relative difference of our implementation with the Benchmark results (on which we could rely) are a bit too large. In some points the relative difference is of the order of  $10^{-4}$  (see A) which is not small enough for a good agreement.

The usage of different matching scales in figures 11 and 12 produce very small error bands, but there is a difference. First the lower matching scales were taken at  $m_c/2$  and  $m_b/2$ . This seemed wrong, because then the PDF has been evolved back from  $m_c$  (the starting scale) to the lower scale  $m_c/2$  which is matched to a higher number of flavors there. Next, the same region is passed in evolving to higher scale but with  $n_f + 1$  light flavors. So therefore the first matching scale has been changed to  $m_c$ . Then the error bands became much smaller.

What can be seen very clearly is that the gluon distribution and the u valance distribution contribute oppositely to fulfill the momentum rule which states that all integrated PDFs give the total momentum fraction of the proton, which is 1.

There are no signals for big mistakes in the matching procedure of the PDFs in the code. All the tests that are performed (comparison with `Maple`, calculating Mellin moments, comparison to Benchmark data) indicate a well performed matching.

## Epilogue

I want to thank my supervisor Markus Diehl for this opportunity and the many discussions we had on the topic of flavor matching and QCD. Also many thanks to Riccardo Nagar for helping me finding my way in c++ and other technical issues. He was also a great help for explaining theoretical issues. I also want to thank the organization of the DESY summer school for a very nice 8 weeks at this institute. It has been a wonderful time.

## References

- [1] Ellis, Webber, Stirling. *QCD and Collider Physics*. Cambridge University Press 8 (1996) 1-435.
- [2] Golec-Biernat, Stasto. *Unintegrated double parton distributions*. Phys. Rev. D 95, 034033 (2017).
- [3] V. Khachatryan *et al.* [CMS Collaboration]. *Measurement of the inclusive 3-jet production differential cross section in proton-proton collisions at 7 TeV and determination of the strong coupling constant in the TeV range*. Eur. Phys. J. C **75** (2015) no.5, 186 [arXiv:1412.1633 [hep-ex]].
- [4] M. Tanabashi *et al.* *Particle Data Group*, Phys. Rev. D 98, 030001 (2018).
- [5] The xFitter Developers' Team. *Impact of the heavy quark matching scales in PDF fits*. arXiv:1707.05343 [hep-ph]
- [6] K.G. Chetyrkin, B.A. Kniehl, M. Steinhauser. *Strong Coupling Constant with Flavour Thresholds at Four Loops in the  $\overline{MS}$  Scheme*. Phys.Rev.Lett. 79 (1997) 2184-2187.
- [7] Weisstein, Eric W. *Series Reversion*. MathWorld—A Wolfram Web Resource. <http://mathworld.wolfram.com/SeriesReversion.html>
- [8] M. Bonvini, A. S. Papanastasiou and F. J. Tackmann, *Resummation and matching of  $b$ -quark mass effects in  $b\bar{b}H$  production*. JHEP **1511** (2015) 196 [arXiv:1508.03288 [hep-ph]].
- [9] M. Buza, Y. Matiounine, J. Smith and W. L. van Neerven. *Charm electroproduction viewed in the variable flavor number scheme versus fixed order perturbation theory*. Eur. Phys. J. C **1** (1998) 301 [hep-ph/9612398].
- [10] A. Behring, I. Bierenbaum, J. Blümlein, A. De Freitas, S. Klein and F. Wißbrock. *The logarithmic contributions to the  $O(\alpha_s^3)$  asymptotic massive Wilson coefficients and operator matrix elements in deeply inelastic scattering*. Eur. Phys. J. C **74** (2014) no.9, 3033 [arXiv:1403.6356 [hep-ph]].
- [11] J. Ablinger, J. Blmlein, A. De Freitas, A. Hasselhuhn, A. von Manteuffel, M. Round, C. Schneider and F. Wissbrock, *The Transition Matrix Element  $A_{gq}(N)$  of the Variable Flavor Number Scheme at  $O(\alpha_s^3)$* . Nucl. Phys. B **882** (2014) 263 [arXiv:1402.0359 [hep-ph]].
- [12] J. Ablinger *et al.*, *The 3-Loop Non-Singlet Heavy Flavor Contributions and Anomalous Dimensions for the Structure Function  $F_2(x, Q^2)$  and Transversity* Nucl. Phys. B **886** (2014) 733 [arXiv:1406.4654 [hep-ph]].

- [13] A. Behring. *Three-loop QCD corrections from massive quarks to deep-inelastic structure functions and operator matrix elements.*
- [14] E. Remiddi and J. A. M. Vermaseren. *Harmonic polylogarithms.* Int. J. Mod. Phys. A **15** (2000) 725 [hep-ph/9905237].
- [15] Lloyd N. Trefethen *Approximation Theory and Approximation Practice.* Society for Industrial and Applied Mathematics Philadelphia, PA, USA ©2012 ISBN:1611972396 9781611972399
- [16] M. Dittmar *et al.*, *Working Group I: Parton distributions: Summary report for the HERA LHC Workshop Proceedings.* hep-ph/0511119.
- [17] W. Giele *et al.*, *The QCD / SM working group: Summary report.* hep-ph/0204316.

## A. VFNS comparison with Benchmark results

The comparison of evolving the metadata set LesHouchesWG2002 in a variable flavor number scheme is given here. In table A, the relative differences from our procedure compared to the Benchmark results are shown. The d valance and gluon distribution at NNLO in point  $x = 10^{-7}$  are most likely typos in table 15 in [16].

$x$	$xu_v$	$xd_v$	$xL_-$	$2xL_+$	$xs_+$	$xc_+$	$xb_+$	$xg$
NLO $n_f = 3$ to 5								
$10^{-7}$	$1.412^{-5}$	$3.270^{-6}$	$4.197^{-6}$	$1.276^{-5}$	$3.965^{-6}$	$5.379^{-6}$	$5.624^{-6}$	$2.301^{-5}$
$10^{-6}$	$3.083^{-6}$	$7.420^{-6}$	$1.573^{-5}$	$4.277^{-6}$	$2.317^{-6}$	$3.986^{-6}$	$1.035^{-6}$	$9.703^{-6}$
$10^{-5}$	$6.065^{-6}$	$2.684^{-5}$	$2.855^{-6}$	$1.220^{-5}$	$1.951^{-5}$	$2.469^{-5}$	$1.891^{-5}$	$1.471^{-5}$
$10^{-4}$	$1.657^{-5}$	$1.582^{-6}$	$6.100^{-6}$	$1.789^{-5}$	$5.814^{-6}$	$9.297^{-7}$	$8.554^{-8}$	$2.077^{-6}$
$10^{-3}$	$1.042^{-6}$	$7.580^{-6}$	$2.565^{-5}$	$8.074^{-7}$	$1.474^{-5}$	$3.494^{-6}$	$1.475^{-5}$	$1.351^{-5}$
$10^{-2}$	$9.249^{-6}$	$2.404^{-5}$	$2.298^{-6}$	$4.511^{-6}$	$4.776^{-6}$	$7.837^{-7}$	$7.891^{-6}$	$6.330^{-6}$
0.1	$3.202^{-6}$	$1.287^{-5}$	$1.747^{-6}$	$9.411^{-6}$	$2.136^{-5}$	$5.122^{-6}$	$1.298^{-5}$	$5.358^{-7}$
0.3	$1.906^{-6}$	$2.445^{-5}$	$5.257^{-6}$	$1.049^{-5}$	$3.349^{-6}$	$8.027^{-6}$	$1.626^{-5}$	$2.695^{-6}$
0.5	$1.692^{-5}$	$1.264^{-5}$	$5.877^{-6}$	$1.391^{-5}$	$2.077^{-6}$	$4.301^{-6}$	$9.578^{-6}$	$3.162^{-6}$
0.7	$7.019^{-5}$	$8.078^{-6}$	$7.935^{-6}$	$6.020^{-6}$	$3.609^{-5}$	$8.442^{-6}$	$5.935^{-6}$	$8.732^{-6}$
0.9	$1.344^{-5}$	$6.752^{-6}$	$1.752^{-5}$	$5.941^{-5}$	$6.495^{-5}$	$1.749^{-4}$	$2.239^{-5}$	$3.351^{-5}$
NNLO $n_f = 3$ to 5								
$10^{-7}$	$1.450^{-5}$	9.000	$3.606^{-6}$	$1.874^{-5}$	$1.124^{-7}$	$5.696^{-6}$	$1.134^{-5}$	$9.000^{-1}$
$10^{-6}$	$5.777^{-6}$	$9.378^{-6}$	$8.332^{-6}$	$6.671^{-6}$	$5.423^{-6}$	$7.896^{-6}$	$5.997^{-6}$	$3.138^{-6}$
$10^{-5}$	$5.843^{-7}$	$2.122^{-5}$	$3.803^{-5}$	$1.007^{-5}$	$2.817^{-5}$	$3.306^{-5}$	$4.372^{-6}$	$6.909^{-6}$
$10^{-4}$	$1.918^{-5}$	$3.472^{-6}$	$3.836^{-6}$	$2.689^{-5}$	$2.551^{-6}$	$4.762^{-6}$	$6.991^{-6}$	$2.618^{-6}$
$10^{-3}$	$3.219^{-6}$	$4.851^{-6}$	$1.591^{-5}$	$6.123^{-7}$	$1.210^{-5}$	$1.278^{-5}$	$1.360^{-5}$	$1.963^{-6}$
$10^{-2}$	$1.903^{-6}$	$9.760^{-6}$	$3.924^{-7}$	$8.060^{-6}$	$1.629^{-6}$	$2.160^{-5}$	$7.031^{-7}$	$5.472^{-6}$
0.1	$2.075^{-6}$	$8.355^{-6}$	$3.340^{-6}$	$8.596^{-6}$	$1.842^{-5}$	$2.467^{-5}$	$6.872^{-6}$	$5.218^{-6}$
0.3	$8.320^{-6}$	$9.436^{-6}$	$1.205^{-5}$	$2.865^{-6}$	$9.518^{-8}$	$6.268^{-5}$	$5.364^{-5}$	$2.803^{-6}$
0.5	$1.422^{-5}$	$1.136^{-5}$	$9.948^{-6}$	$3.676^{-6}$	$3.371^{-6}$	$1.726^{-4}$	$8.162^{-5}$	$9.685^{-7}$
0.7	$9.540^{-6}$	$1.660^{-5}$	$2.568^{-5}$	$1.428^{-6}$	$2.559^{-5}$	$3.556^{-4}$	$1.937^{-4}$	$3.863^{-6}$
0.9	$4.496^{-6}$	$4.003^{-6}$	$5.816^{-5}$	$1.784^{-4}$	$1.979^{-5}$	$5.418^{-6}$	$1.456^{-4}$	$2.107^{-6}$

Table 1: Relative difference with evolution benchmark values VFNS.